Hindawi Publishing Corporation
International Journal of Photoenergy
Volume 2011, Article ID 259453, 10 pages
doi:10.1155/2011/259453

Research Article

Selective Photooxidation and Photoreduction Processes at TiO_2 Surface-Modified by Grafted Vanadyl

Rossano Amadelli,[1] Luca Samiolo,[1] Andrea Maldotti,[2] Alessandra Molinari,[2] and Delia Gazzoli[3]

[1] *CNR-ISOF, U.O.S. of Ferrara, c/o Department of Chemistry, University of Ferrara, Via L. Borsari 46, I-44121 Ferrara, Italy*
[2] *Department of Chemistry, University of Ferrara, Via L. Borsari 46, I-44121 Ferrara, Italy*
[3] *Department of Chemistry, University of Rome "La Sapienza", Piazzale Aldo Moro 5, I-00185 Rome, Italy*

Correspondence should be addressed to Rossano Amadelli, amr@unife.it

Received 16 May 2011; Revised 27 July 2011; Accepted 27 July 2011

Academic Editor: Ignazio Bellobono

Titanium dioxide was surface-modified by grafting vanadyl species using vanadyl triisopropoxide as a precursor. The resulting material, $(VO_x)_n/TiO_2$, was characterized by Raman spectroscopy and photoelectrochemical methods. Photocatalytic oxidation of benzyl alcohol and cyclohexene were used to test oxidation selectivity and 4-nitro-benzaldehyde to assess selective photoreduction. The surface-modified TiO_2 exhibits an enhanced selectivity to benzaldehyde in the photocatalytic oxidation of benzyl alcohol in an aqueous medium and an increase of cyclohexenol formation in the case of cyclohexene in nonaqueous solvent. The salient result is the 100% selective reduction of the nitrogroup in 4-nitro-benzaldehyde achieved under mild experimental conditions.

1. Introduction

Photoelectrocatalysis on semiconductors is now an important research field, largely because of attractive applications in environment remediation [1–3]. Related applications in organic syntheses have equally attracted large interest [4–7] already from the infancy of the studies on photoelectrocatalysis, some thirty years ago [8].

In both disciplines, titanium dioxide is by far and large the most widely employed photocatalyst by reason of its unique characteristics. It is, however, a UV light absorber and, understandably, the need to shift its absorption edge into the visible region has spawned new research focusing on the modification of physical properties, particularly the width of the bandgap. This is done mainly by cations or anions doping [9–12], but in recent developments it is proposed that also grafting of metal complexes [13] or simple cations on the TiO_2 surface enhances visible light absorption [14, 15].

Visible light absorption is not the sole scope of surface modification and, in fact, targeted changes in the interfacial reactivity of substrates is also an important issue; the case of sulfated TiO_2 [16] is a good example. In the particular case of photocatalysis for synthetic processes, the specific need of products selectivity has stimulated research on molecular functionalization of surfaces. In this connection, research has been far more intense in the field of electrocatalysis with modified electrodes [17] than in the related relatively younger branch of photoelectrocatalysis.

It is sometimes stated but more often implied that the goal of surface functionalization is tailoring the surface to introduce new surface sites or modify the existing ones so as to meet specific needs, including a control of the interface. It is expected that this can lead to reaction intermediate(s) accumulation instead of complete oxidation. Such a goal is essentially described by the concept of *site isolation* introduced several years ago by Grasselli [18]. The term indicates that a selective reaction to partial oxidation product requires a surface arrangement that limits the attack on the adsorbed intermediate, so that desorption of partially oxidized species is faster than its consecutive oxidation and degradation. One example of such approach is described in our earlier work on TiO_2 modified with Fe-porphyrins [4].

An impressive amount of work is available on oxide surfaces grafted with vanadium species in view of use as catalysts in thermal catalysis [19, 20]. By comparison, the studies in photocatalysis are less numerous and largely devoted to VO_x on SiO_2 or Ti-modified SiO_2 supports [21, 22].

Herein we examine the photochemical behavior of vanadyl-modified TiO_2 electrodes and particle suspensions. From the morphological point of view, the vanadyl overlayer is constituted of hydrated species since, at this stage of the research, the catalyst was not calcined in order to avoid surface doping by vanadium. As concerns the photocatalytic activity of the grafted TiO_2, our interest focuses on intermediates formation and accumulation in the photooxidation of benzyl alcohol and cyclohexene as well as in the process of 4-nitrobenzaldehyde photoreduction.

2. Experimental

2.1. Materials and Equipment. All chemicals were Sigma-Aldrich or Fluka spectroscopic grade reagents and used as received, except hexane which was dehydrated by standard methods. Titanium dioxide P-25 from Degussa was employed in all experiments.

The ICP-AES analytical determinations of vanadium, using its spectral line at 292.4 nm, were carried out on a Perkin-Elmer Model OPTIMA 3100 XL spectrometer equipped with segmented array charge-coupled device (SCD) detector.

Raman spectra were collected on powder samples at room temperature in the back-scattering geometry with an inVia Renishaw spectrometer equipped with an air-cooled CCD detector and a super-Notch filter. The emission line at 488.3 nm from an Ar^+ ion laser was focused on the sample under a Leica DLML microscope using a 20× objective. Five 20 s accumulations were acquired for each sample with a power of the incident beam on the sample of about 5 mW. The spectral resolution was 2 cm^{-1} and the spectra were calibrated using the 520.5 cm^{-1} line of a silicon wafer.

Gas chromatographic analyses of photooxidation products of benzyl alcohol and cyclohexene were carried out using an HP6890 Series instrument equipped with a flame ionization detector and an HP-5 capillary column. Quantitative analysis was performed with calibration curves obtained with authentic samples.

Photoreduction of 4-nitrobenzaldehyde was followed by HPLC. Measurements were conducted on a Thermo Separation Products instrument equipped with a SpectroMonitor 5000 detector, using a Econosphere C18 5 micron column. A 30/70 % acetonitrile/water was used as mobile phase at a costant flux of 0.45 mL min^{-1}.

UV-visible spectra of solutions were recorded on a Kontron spectrophotometer (Uvikon 943), using a 2 mm quartz cell. Diffuse reflectance UV-visible spectra (DRS) were recorded at room temperature on a JASCO V-570 spectrophotometer equipped with an integrating sphere and $BaSO_4$ was used as reference. The Kubelka-Munk function $F(R) = (1 - R)^2/2R$ was obtained from reflectance to approximate the optical absorbance.

The ESR experiments were performed with a Bruker 220 SE spectrometer at a microwave frequency of 9.4 GHz. Aqueous suspensions of sample with the hole acceptor were put into a flat quartz cell and directly irradiated into the ESR cavity at room temperature. No ESR signals were observed in the dark and during irradiation of solutions of radical trap/alcohol in the absence of TiO_2. In ESR spin trapping experiments, we used phenyl-tert-butylnitrone (PBN) as the radicals trap.

Photoelectrochemical experiments were done using an EG&G model 273A potentiostat-galvanostat with EG&G software. A conventional three-compartment glass cell was employed where the working electrode compartment had an optical window for illumination. The counter electrode was a Pt sheet and saturated calomel (SCE) was used as a reference electrode.

Illumination source was a mercury medium pressure lamp (Helios Italquartz) equipped with $\lambda > 360$ nm cut-off filter. The intensity of light was 15 mW cm^{-2}, measured with a Newport instrument (Power Meter 1918c).

An important, necessary information concerns the possible loss of vanadium from the surface during photocatalytic experiments. We checked this after 6 h irradiation and found that less than 1/1000 of the quantity initially present on the surface of the photocatalyst is detached. Then an excellent stability of grafted vanadium can be claimed during prolonged irradiation in nonaqueous as well as aqueous media.

2.2. Methods. The catalysts were prepared by grafting vanadyl triisopropoxide, $OV(OR)_3$ (Aldrich), dissolved in anhydrous n-hexane (Fluka) on TiO_2 (Degussa, P-25). The reaction was carried out under inert atmosphere, at 25°C, for 18 h. The solid was then recovered by centrifugation, washed with n-hexane, and after removing the solvent, it was resuspended in water for 7 h in order to hydrolyse the grafted vanadyl and remove residual isopropyl groups coordinated to vanadium. Finally, after centrifugation, the powder was dried in an oven at 100°C for 24 hours. For comparison, TiO_2 was also treated in the same way but in the absence of added vanadium precursor. The amount of supported vanadium has been determined by ICP-AES after dissolving the sample with a solution of H_2O_2 and NaOH.

Electrodes were prepared from the TiO_2 powder on Ti following the procedure of films preparation described previously [23]. Vanadium modified electrodes were prepared by immersing the film in a 6×10^{-4} mol L^{-1} solution of $OV(OR)_3$ in n-hexane for 30 minutes. The electrode was then washed in pure hexane to remove residual precursor not bounded to TiO_2 surface and finally hydrolysed.

Photocatalytic experiments with suspensions were conducted in Pyrex semicylindrical reactors with a flat window, containing the test solution and the photocatalyst in an amount of 4 g L^{-1}. During experiments, the solution was stirred with a Teflon-covered magnetic bar. All experiments have been carried out at room temperature (298 ± 1 K). Oxygenation of the solution was assured by maintaining the reactor under pure O_2 at 1 atm. No detectable oxidation products were obtained when blank experiments were run in

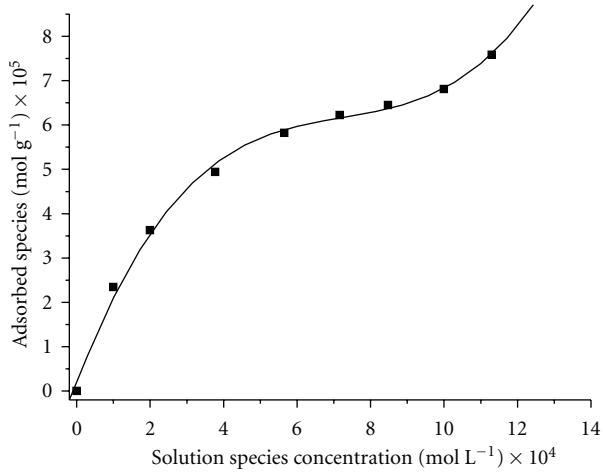

FIGURE 1: Surface concentration of vanadium as a function of vanadyl triisopropoxide in 0.03 L n-hexane containing 0.1 g TiO_2 (Degussa P-25). Details are described in the experimental section.

the dark or upon irradiation of the starting alcohol solutions in the absence of the photocatalysts.

For the experiments of nitroaromatics reduction, solutions were deaerated with argon.

3. Results and Discussion

3.1. Materials Characterization. Results of $OV(OR)_3$ uptake by TiO_2 are displayed in Figure 1. The plot of the surface concentration versus the initial concentration in the solution shows a qualitative Langmuirean behavior, with a short plateau being reached for an $OV(OR)_3$ concentration in solution of 8×10^{-4} mol L^{-1}. Above this value, the surface concentration starts to rise again, likely indicating the beginning of a multilayer growth due to a preferential interaction of incoming molecules with already adsorbed vanadium species.

Taking the average value of 50 m^2 g^{-1} for the surface area of TiO_2, calculations yield 0.95 vanadium atoms nm^{-2} in the plateau region (Figure 1), which is in excellent agreement with 1.05 atoms nm^{-2} obtained from ICP-AES analysis. This value corresponds to ~1/4 of the reported surface concentration of OH groups (4.6–4.8 per nm^2) [24] that are the binding sites. According to Wachs [25], a monolayer of vanadium on various oxides including TiO_2 generally corresponds to 4-5 atoms nm^{-2}, although it is to be remarked that other literature reports are rather vague on the concept of monolayer formation by vanadium species on titania.

Photocatalysis tests have been carried out with TiO_2 samples modified with either 6×10^{-5} mol g^{-1} (henceforth sample V1) or 2×10^{-5} mol g^{-1} vanadium (henceforth sample V2), that is, in the plateau region or in the rising part of the adsorption curve, respectively.

Diffuse reflectance measurements (spectra not displayed) showed that the optical absorbance at 360 nm for sample V1 is twice compared to the parent unmodified TiO_2. The spectra also feature a similar increase between 400 and 450 nm which can be assigned to absorption by hydrated, octahedric coordinated vanadium species [26].

An insight into the molecular structure of the vanadyl-grafted species has been achieved by Raman spectroscopy, which alone or in combination with FTIR spectroscopy offers a widely recognized tool to identify the various vanadium species (isolated and/or polyvanadyl chains) that can be formed at the sample surface depending on the amount of vanadium precursor, the nature of the support, and the preparation method [20, 27]. For different supported metal oxide systems, Raman bands in the range between 950 and 1050 cm^{-1} are assigned to the stretching mode of the short terminal M=O bonds, whereas bands in the range between 500 and 950 cm^{-1} are attributed to either the antisymmetric stretch of M–O–M bonds or the symmetric stretch of $(–O–M–O–)_n$ bonds of polymerized entities [28–30]. It is noteworthy that the Raman signals we observed cannot be directly compared with those of vanadium species in solution because grafting takes place in nonaqueous medium by a condensation process between surface OH groups and $(RO)_3V{=}O$ with formation of chemical bonds that, once formed, are stable even in an aqueous medium (Section 2.1). The concentration of grafted VO_x in this paper corresponds to a fraction of a monolayer, and if the degree of dispersion of the chemically bound VO_x species is high, oligomerization is expected to be low also on account of the lack of surface mobility of the anchored molecules. On this basis, assignment of a Raman band at 985 cm^{-1} to surface clusters of the type $(V_{10}O_{28})$ [25, 30] can be safely excluded. Additionally, surface immobilized oxovanadyl experiences changes in the symmetry with respect to free species in solution, and thus broadening and shifting of the Raman bands can be expected.

Both samples V1 and V2 exhibited, under ambient conditions, bands in the range 130–800 cm^{-1} due to TiO_2 modifications and a composite feature spanning the frequencies range 850–1050 cm^{-1} due to vanadium species (Figure 2). Vanadium species contributing below 800 cm^{-1} are obscured by the scattering from the TiO_2 support.

Spectral analysis disclosed peaks due to anatase (about 140, 400, 520 and 639 cm^{-1}) and rutile (about 235, 450, 520, 612, and 805 cm^{-1}) TiO_2 [31], whereas the complex VO_x band, resolved by curve-fitting procedures, resulted with components at about 940–950 cm^{-1} and at about 980–1000 cm^{-1} and with a very broad feature centered at about 860 cm^{-1}. The higher frequency band may be assigned to V=O stretching vibrations within monomeric vanadyl species [25], the other two bands to stretching of the V=O internal mode and V–O–V modes within polymeric structures. As expected, a comparison of the spectra of sample V2 and V1 (Figure 2, curves a, b) reveals a slightly higher amount of oligomeric species for the sample with the higher VO_x surface concentration.

In the forthcoming discussion, the vanadyl/TiO_2 catalyst is more properly described by $(VO_x)_n/TiO_2$, where n refers to formation of oligomers as indicated by the Raman results.

3.2. Photoelectrochemistry. The grafted vanadyl species can induce surface states with energy levels lying within

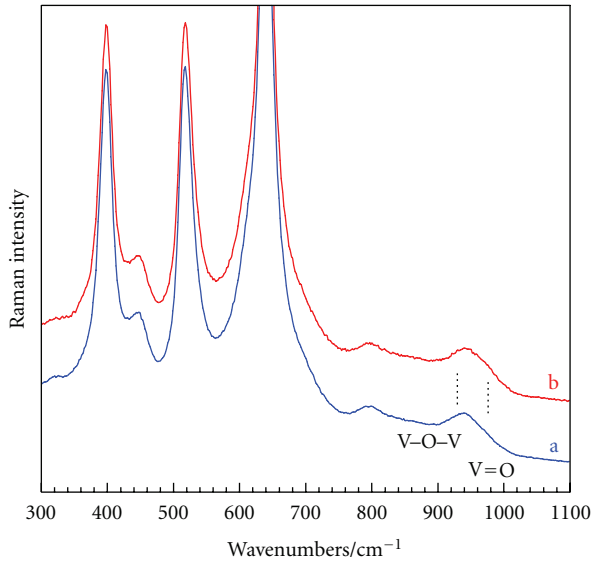

FIGURE 2: Raman spectrum for vanadyl-modified TiO_2 samples. Curve (a), 2×10^{-5} vanadium mol per gram of TiO_2 (sample V2); curve (b), 6×10^{-5} vanadium mol per gram of TiO_2 (sample V1).

the bandgap and thus can possibly control recombination of photogenerated charges and interfacial charge transfer. Photoelectrochemical measurements provide invaluable information on their occurrence and additionally on important parameters such as the flat band potential (V_{fb}).

The measurement of V_{fb} can be carried out by different methods, although it is commonly evaluated from Mott-Schottky (MS) plots constructed from capacity data [32]. In the present case, MS plots for the case of unmodified TiO_2 in 1 mol L^{-1} $NaClO_4$ gave a straight line from which a V_{fb} value of -0.75 V was obtained. Derivatization with vanadyl species resulted in more complicated MS plots where two regions of linearity were detected, extrapolating at -0.65 V and -0.2 V. Actually, according to Dean and Stimming [33], evaluation of V_{fb} from Mott-Schottky plots is not straightforward in the case of semiconductors with a wide band of localized states, since results are often misleading. We then used the alternative V_{fb} evaluation from the measurement of the open circuit potential decay in the dark and under strong illumination of the electrode [34]. Results displayed in Figure 3(a) show that, for the pristine electrode, the open circuit potential under illumination stabilizes at -0.72 V, in very good agreement with MS results. Conversely, the curves of Figure 3(b) for $(VO_x)_n/TiO_2$-modified electrodes feature an arrest of the potential decay around -0.2 V for a length of time that is clearly connected to the amount of surface vanadium; afterwards, the potential decays more or less slowly to more negative values. This behavior can be reasonably attributed to filling of surface states by photogenerated electrons and, upon completion of this process, a negative shift of the Fermi level toward flat-band condition occurs.

This surface state, located about 0.5 V below the conduction band, can be identified with V^V that is reduced to V^{IV} on illumination and, indeed, this conclusion is confirmed by the ESR spectra shown in the inset of Figure 3(b). These data are obtained at room temperature using a powder catalyst (then under analogous open circuit conditions) and reveal that illumination causes the appearance of the ESR spectrum typical of V^{IV}; it disappears in the presence of O_2, in keeping with the known facile reoxidation of the reduced vanadium center to V^V.

In electrochemical experiments with vanadium species deposited on rutile electrodes, Haber and Novak [35] identified the V^V/V^{IV} couple at more positive potentials. Actually, their electrodes were prereduced in hydrogen to increase conductivity while ours were prepared from slurries (see Section 2) and then are considerably less doped and conductive. The lower number of electrons can then be the cause of the observed shift or reduction to lower potentials.

Photoelectrochemical measurements are often helpful in the elucidation of processes both at electrodes and, indirectly, at semiconductor powder suspensions. In particular, a straightforward separate analysis of cathodic and anodic processes is possible.

An example of photocurrent versus time transients is given in Figure 4(a) for a $(VO_x)_n/TiO_2$ electrode in an aqueous neutral solution containing 2-propanol as a test oxidizable substrate. It is seen in this plot that the current in the dark is zero, while an oxidation photocurrent is recorded both in the absence (curve 1) and in the presence of 2-propanol (curve 2). In the latter case, one notices a rather delayed onset of alcohol oxidation, and the photocurrent then slowly reaches a steady-state value of $\sim 45\,\mu$A. This current is about eight times lower than that measured with an unmodified TiO_2 electrode under the same experimental conditions, and one obviously concludes that the photoelectrooxidation process is comparatively inefficient. The phenomena can be ascribed to a decrease of light absorption by TiO_2 (*vide supra*) and to a sluggish interaction of hole acceptor with the surface, leading to increased recombination possibly at V^V centers.

The background photocurrent observed in the neat electrolyte (curves 1 in Figures 4(a) and 4(b)) presents interesting aspects that are worth some comments: (i) it depends on the amount of surface vanadium and has a magnitude of $\sim 15\,\mu$A for the conditions described in Figure 4; (ii) it decreases progressively for irradiation wavelengths $\lambda > 360$ nm; (iii) it decreases to zero at potentials more negative than -0.2 V (Figure 4(a), curve 1). These facts are suggestive of an involvement of the $(VO_x)_n$ overlayer in determining the electrode behavior in the absence of the hole acceptor. In particular, one notices that at potentials below -0.2 V, vanadium is present as V^{IV} (*vide supra*) and it is then natural to associate the anodic background photocurrent with phenomena connected to absorption of light by the $(VO_x)_n$ that brings about reduction of V^V to V^{IV}. This transfer of electrons through the external circuit might bear some analogy with the increase of TiO_2 conductivity reported in thermal studies on V_2O_5/TiO_2 [36], attributed to creation of bond unsaturations in the vanadium oxide deposit. We cannot advocate a similar explanation, because, in our case, the $(VO_x)_n$ overlayer does not possess the characteristics of phase oxides as in the cited work. As

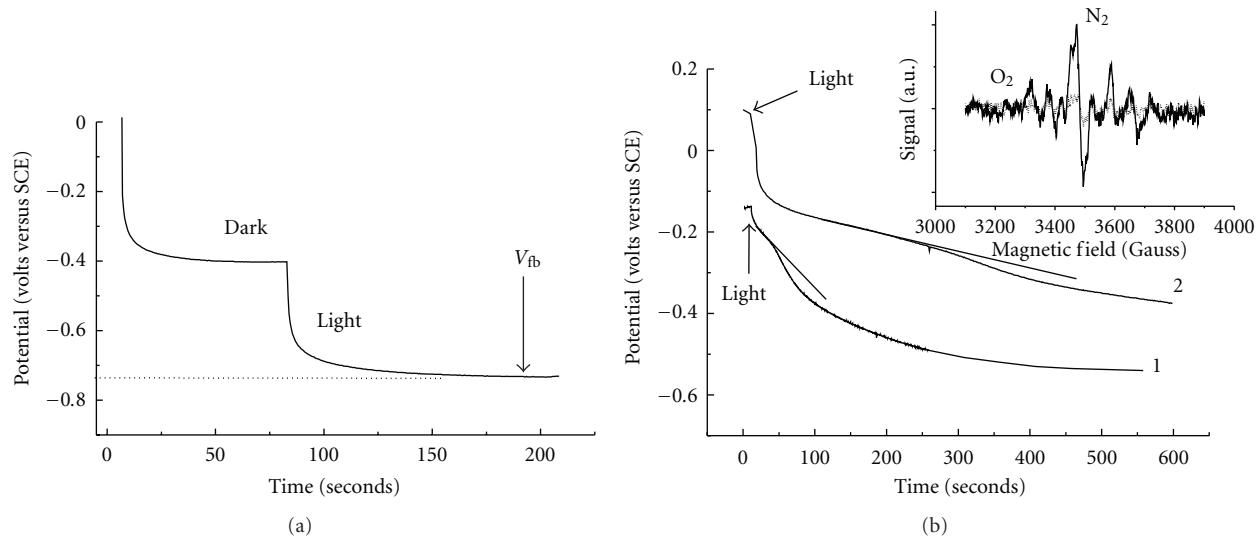

FIGURE 3: Open circuit potential decay as a function of time for illuminated electrodes: (a) TiO_2 and (b) $(VO_x)_n/TiO_2$, where the amount of vanadium loaded on TiO_2 is 3×10^{-7} mol (curve 1) and 5.6×10^{-7} mol (curve b). Electrode area: 1.1 cm^2. Supporting electrolyte: 1 mol L^{-1} $NaClO_4$. Irradiation: $\lambda > 360$ nm. The inset in graph (b) refers to ESR spectra recorded on $(VO_x)_n/TiO_2$ powders illuminated at $\lambda > 360$ nm in the presence of 0.1 mol L^{-1} HCOONa (see text for explanation), in the absence and in the presence of oxygen.

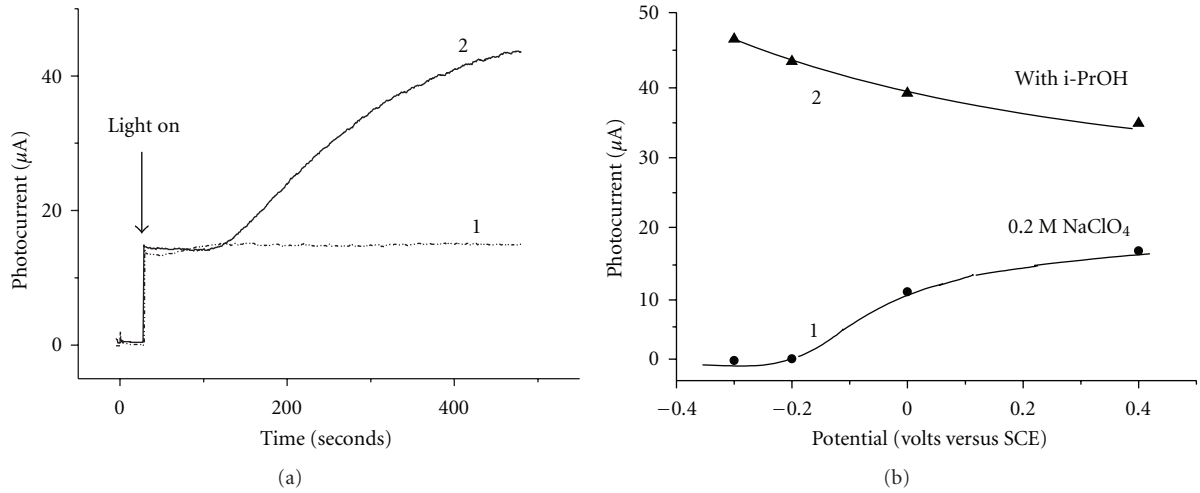

FIGURE 4: Graph (a) shows photocurrent versus time curves for a $(VO_x)_n/TiO_2$ electrode in a 1 mol L^{-1} $NaClO_4$ aqueous solution, in the absence (curve 1) and in the presence (curve 2) of 0.2 mol L^{-1} 2-propanol. Graph (b) shows the potential dependence of photocurrents for a $(VO_x)_n/TiO_2$ electrode in 1 mol L^{-1} $NaClO_4$ in the absence (curve 1) and in the presence (curve 2) of 0.2 mol L^{-1} 2-propanol in water. The amount of vanadium on the TiO_2 film is 3×10^{-7} mol. Electrode area: 1.1 cm^2. Irradiation: $\lambda > 360$ nm.

an alternative explanation we advance the possibility that electrons can be released into TiO_2 from the $(-V^{IV}-O^-)^*$ excited states [37].

The fact that V^{IV} provides active sites for photooxidation processes is not just surmised but corroborated by other experimental evidence coming again from results of 2-propanol photoelectrochemical oxidation. We mentioned above that this process is delayed in time (Figure 4(a)) and, in this connection, we found that the delay depends on electrode pre-reduction. No delay in the photooxidation of 2-propanol was observed if the electrode is pre-treated at –0.4 V for a length of time that ensures reduction of V^V. Moreover, photocurrents versus potentials for the oxidation of 2-propanol are actually higher at $E < -0.2$ V when V^{IV} is stable (Figure 4(b)), which seemingly agrees with literature reports that identify V^{IV} as the active centers for adsorption of 2-propanol [38].

It was also surprising that no alcohol photooxidation was observed in CH_3CN but just the same background photocurrent that is also recorded in an aqueous medium (Figure 4(a), curve 1). This behavior can possibly be explained by competition for active sites since it is known that acetonitrile

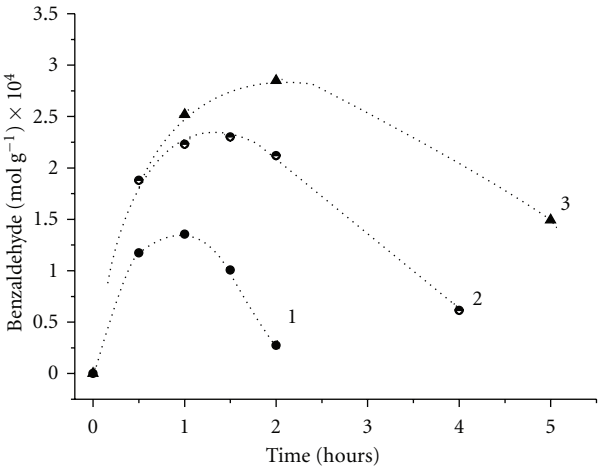

FIGURE 5: Benzaldehyde formation as a function of time during the photooxidation of 1×10^{-3} mol L^{-1} benzyl alcohol in aqueous suspensions of TiO_2 (curve 1), $(VO_x)_n/TiO_2$ (2×10^{-5} mol g^{-1} vanadium, curve 2), and $(VO_x)_n/TiO_2$ (6×10^{-5} mol g^{-1} vanadium, curve 3). Irradiation: $\lambda > 360$ nm. I = 15 mW cm^{-2}.

is strongly adsorbed at vanadium sites due to their Lewis acidity [39].

3.3. Photocatalysis. The photocatalytic activity of the $(VO_x)_n/TiO_2$ system was investigated using simple organic molecules such as benzyl alcohol and cyclohexene to test selectivity in photooxidation and 4-nitrobenzaldehyde to assess selective photoreduction.

3.3.1. Photooxidation of Alcohols. Formation of benzaldehyde from benzyl alcohol has an applied interest and is widely used to probe selective photooxidation on TiO_2 [12, 40, 41]. Results reported in Figure 5 show the formation of benzaldehyde as a function of irradiation time for $(VO_x)_n/TiO_2$ and unmodified TiO_2 in water. Upon continued irradiation, benzyl alcohol gives benzaldehyde which is subsequently photooxidized to benzoic acid and further. It is clearly seen that accumulation of benzaldehyde is favored on $(VO_x)_n/TiO_2$ to an extent that depends on the concentration of surface vanadium species; it reaches a maximum of 30% of the initial alcohol concentration for sample V1, corresponding to a concentration in the plateau region of Figure 1. Selectivity is only 14% for the bare TiO_2. Reactions do not proceed in the absence of O_2 or by irradiation with visible light. Moreover, we observed no photocatalytic activity with Al_2O_3 grafted with the same amount of vanadium species (mol m^{-2}) used with TiO_2, and it is concluded that bandgap irradiation plays an important role in the overall oxidation process.

The photocatalytic alcohol oxidation has common features with the photoelectrochemical process discussed above although other aspects of the mechanism are different. It is similar to the condition of an electrode at open circuit with reduction of V^V to V^{IV} by conduction band electrons and through light absorption by ($-V^V=O$) to yield ($-V^{IV}-O$)*. Oxygen is then needed to restore vanadium in its original V^V state and acts as a scavenger of extra conduction band electrons; it has then a key role in the overall process as with bare TiO_2.

In the absence of a diagnostic tool as photocurrent, ESR spin-trap spectroscopy provides a valuable help in the identification of mechanism details on suspensions [42]. We chose again 2-propanol as a relatively simple model alcohol substrate because it can be easily studied by the ESR spin trapping technique. In nonaqueous medium, we observed that upon irradiation of both TiO_2 and $(VO_x)_n/TiO_2$ (<600 s), a triplet of doublets signal appears (not shown) with hyperfine splitting constants $a_N = 14.5$ G and $a_H = 2.7$ G, assigned to trapped alkoxy-radical ($R_2-CHO^\bullet$) on the basis of tabulated data [43]. With $(VO_x)_n/TiO_2$, however, the intensity of the ESR signal of the adduct is about twice lower than observed with pristine TiO_2, which might be interpreted as another evidence that alcohols interact with the surface [44, 45] and that the presence of $(VO_x)_n$ sites apparently influence the overall adsorption on the bare TiO_2 [44]. Results can also be explained by a slower desorption of the radical formed from alcohol preferentially coordinated to vanadium centers. This kind of mechanism has been proposed in thermal catalysis studies [46] and, significantly, in a recent work by Ciambelli et al. [47] on the selective gas-phase photooxidation of ethanol at vanadium-modified TiO_2, it is proposed that Ti–O–V and V–O–V functionalities are the selective oxidation sites.

An earlier article by Carlson and Griffin [48] on the oxidation of methanol is a much cited one but their experimental conditions are conspicuously different from ours. For example, their preparation involves a final calcination at 723 K and this leads to doping as clearly stated in a more recent article by Herrmann and Disdier [36]. Additionally, the vanadium surface concentration in our work is 1 V/nm^2, that is, 1×10^{14} V/cm^2 while Carlson and Griffin report a value of 10×10^{14} V/cm^2, and it is not surprising that, even neglecting doping, they observe blocking effect and not the site cooperation that we are proposing.

In analogous EPR spin-trapping experiments in aqueous medium we found that the trapped species detected is the hydroxy-alkyl radical ($R_2-^\bullet COH$) as inferred from the triplet of doublets with hyperfine splitting constants $a_N = 15.5$ G and $a_H = 3.6$ G [43, 49]. Since this radical is formed by rearrangement of the primary alkoxy-radical, the fact that it is the only trapped species is an indication that the aqueous medium limits adsorption due to an alcohol-solvent competition for active sites, in agreement with the conclusions of photoelectrochemical data discussed in Section 3.2.

3.3.2. Cyclohexene Photooxidation. Results of cyclohexene photooxidation in nonaqueous medium are given in Table 1 with emphasis on alcohol versus ketone formation. We did not observe detectable amounts of the epoxide. Results are not outstanding as concerns both the total amount of intermediates accumulated and their relative distribution. The increase of ratio of alcohol to ketone for $(VO_x)_n/TiO_2$ compared to the original oxide support can be singled out.

Table 1: Formation of oxygenated intermediates from cyclohexene photooxidation in TiO_2 P-25 and $(VO_x)_n/TiO_2$ dispersed in cyclohexene/CH_2Cl^2 1 : 3. Irradiation at $\lambda > 360$ nm for 2 h in the presence of oxygen. The amount of grafted vanadium was 6×10^{-5} mol g^{-1}. I = 15 mW cm^{-2}.

Catalyst 4 g L^{-1}	Cyclohexenone (mol L^{-1}) $\times 10^3$	Cyclohexenol (mol L^{-1}) $\times 10^3$	Peroxides (mol L^{-1}) $\times 10^3$	Alcohol/ketone
TiO_2 P-25	19.2	9.2	2.82	0.48
$(VO_x)_n/TiO_2$	17.2	14.5	2	0.84

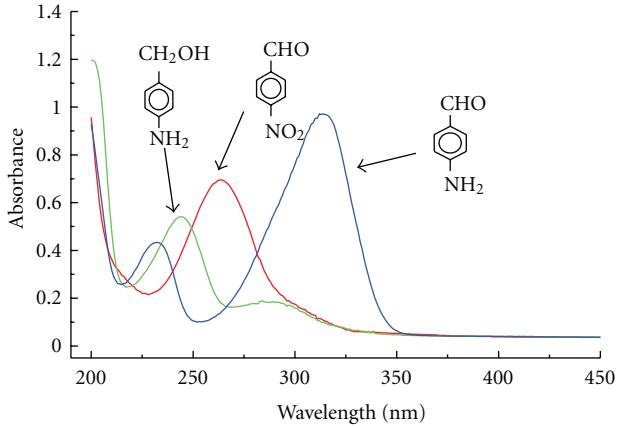

Figure 6: UV-visible spectra illustrating products formation following 1 h irradiation ($\lambda > 360$ nm, I = 15 mW cm^{-2}) of deaerated suspensions of TiO_2 (4 g L^{-1}) and $(VO_x)_n/TiO_2$ (6×10^{-5} mol g^{-1} vanadium) in water/2-propanol (80/20%) containing 0.2×10^{-3} mol L^{-1}4-nitrobenzaldehyde. Results show complete reduction to 4-amino-benzyl alcohol (TiO_2) and 100% selective partial reduction to 4-amino-benzaldehyde $(VO_x)_n/TiO_2$.

The behavior might be explained by a pathway that involves an initial extraction of an allylic hydrogen yielding a radical that reacts with O_2 to give cyclohexenyl peroxide.

Photooxidation of cyclohexene to cyclohexenone on vanadium/silica catalysts has been reported by Mul et al. [50] who found that the reaction proceeds via interaction of cyclohexenyl hydroperoxide with a vanadium center. In the present case, possible cyclohexenyl hydroperoxide intermediates should be characterized with different reactivity since formation of the alcohol predominates. Actually, if peroxo species are involved, formation of products depends very much on the type of bond (covalent or ionic) formed with the vanadium center [51]. The data reported here are very strongly reminiscent of a solution phase autoxidation of cyclohexenyl peroxide formed by a primary step involving reaction of cyclohexenyl radicals with O_2 or O_2^- [42].

3.3.3. Photoreduction of Nitroaromatics. Compared with the photooxidation processes described above, photoreduction of 4-nitrobenzaldehyde on $(VO_x)_n/TiO_2$ provided a more spectacular example of selectivity. We have chosen to test the reduction of a nitroaromatic compound because it is a process of high interest [52].

Apparently, the focus of several publications on the photoreduction of nitroarenes is the selective formation of the corresponding amino-compounds [53]. Formation of the final anilines involves various reduction intermediates [54] and we have shown earlier that these photoreduction intermediates can be building blocks for the synthesis of interesting fine chemicals [55].

Irradiation of deaerated suspensions of $(VO_x)_n/TiO_2$, using 2-propanol as the oxidizable species, led to the formation of 4-amino-benzaldehyde with 100% selectivity. On the contrary, quantitative formation of the 4-amino-benzyl alcohol was observed using the commercial unmodified semiconductor. Results are illustrated by the UV-visible spectra displayed in Figure 6. The spectra of the parent compound and those of the products of its photoreduction are well separated, allowing qualitative as well as quantitative analyses. However, formation of products (4-amino-benzaldehyde and 4-amino-benzyl alcohol) was also checked by HPLC as described in Section 2.1.

It should be mentioned that reduction of 4-nitro-benzaldehyde to 4-amino-benzaldehyde with a chemoselectivity of 98% has also been reported using surface-modified TiO_2 by noble metals [56]. These thermal catalysis studies are carried out in an autoclave at high temperature in tetrahydrofuran, that is, under conditions that are far more severe than those of the present work. We can claim that our approach is closer to Green Chemistry requirements, and our study encourages perspective further research using different nitroarenes as well as other substituted aromatic compounds.

Based on the results presented so far in this paper, there is reason to think that selective reduction of the nitrogroup is due to control of the number of photogenerated electrons. We verified that reduction of 4-nitrobenzaldehyde on glassy carbon takes place at ~ -0.65 V and its reduction by conduction band electrons can take place at TiO_2, as indeed observed. At $(VO_x)_n/TiO_2$ charge transfer on the whole is slower and electrons can be transferred to 4-nitrobenzaldehyde through the V^V/V^{IV} surface state of the $(VO_x)_n$ overlayer. 4-nitrobenzaldehyde can reasonably interact with this hydroxylated layer through the acidic V–OH groups [39]. This situation, depicted in Scheme 1, obviously needs the support of a separate investigation.

4. Conclusions

This paper explores the possibility to obtain site cooperation in the photocatalysis by TiO_2 (Degussa P-25) grafted with vanadyl species. Raman spectroscopy analysis reveals that the $(VO_x)_n$ overlayer consists of hydroxylated/hydrated species,

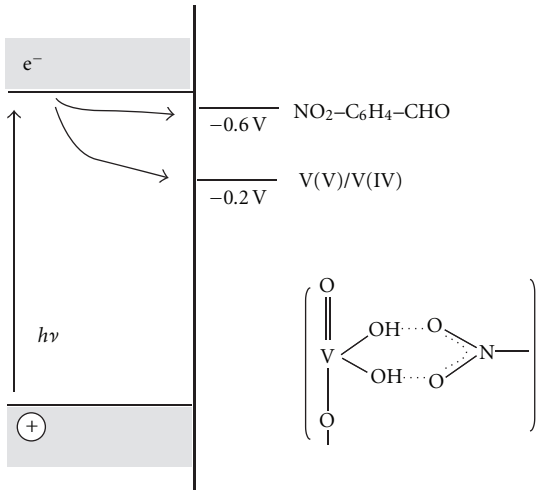

Scheme 1: Energy band diagram illustrating 4-nitrobenzaldehyde photoreduction and the possible interaction of the nitrogroup with the acidic V–OH groups of $(VO_x)_n/TiO_2$.

as expected since the samples were not calcined to avoid surface doping by vanadium.

To the best of our knowledge, we present for the first time results on the photoelectrochemical behavior of a surface-modified $(VO_x)_n/TiO_2$ material. They reveal the presence of a surface state at ~0.5 V below the conduction band that is identified with the V^V/V^{IV} couple. The system presents all the difficulties that are involved in the examination of a composite photocatalysts where the single components taken separately are photoactive. However, by photoelectrochemical and EPR spin-trapping measurements, using 2-propanol as a test compound, we can conclude that the photooxidation process is slower on $(VO_x)_n/TiO_2$ than on bare TiO_2. The causes are a limited interaction of the alcohol with the surface and charge recombination.

The surface-modified TiO_2 features an enhanced selectivity to benzaldehyde in the photocatalytic oxidation of benzyl alcohol in an aqueous medium. Selective reduction of the nitrogroup in 4-nitrobenzaldehyde is the best achievement of this investigation on the photocatalysis by $(VO_x)_n/TiO_2$ and is stimulus to further research in this direction.

References

[1] A. G. Agrios and P. Pichat, "State of the art and perspectives on materials and applications of photocatalysis over TiO_2," *Journal of Applied Electrochemistry*, vol. 35, no. 7-8, pp. 655–663, 2005.

[2] P. Pichat, J. Disdier, C. Hoang-Van, D. Mas, G. Goutailler, and C. Gaysse, "Purification/deodorization of indoor air and gaseous effluents by TiO_2 photocatalysis," *Catalysis Today*, vol. 63, no. 2–4, pp. 363–369, 2000.

[3] H. Zhang, G. Chen, and D. W. Bahnemann, "Photoelectrocatalytic materials for environmental applications," *Journal of Materials Chemistry*, vol. 19, no. 29, pp. 5089–5121, 2009.

[4] A. Maldotti, A. Molinari, and R. Amadelli, "Photocatalysis with organized systems for the oxofunctionalization of hydrocarbons by O_2," *Chemical Reviews*, vol. 102, no. 10, pp. 3811–3836, 2002.

[5] G. Palmisano, V. Augugliaro, M. Pagliaro, and L. Palmisano, "Photocatalysis: a promising route for 21st century organic chemistry," *Chemical Communications*, no. 33, pp. 3425–3437, 2007.

[6] Y. Shiraishi and T. Hirai, "Selective organic transformations on titanium oxide-based photocatalysts," *Journal of Photochemistry and Photobiology C*, vol. 9, no. 4, pp. 157–170, 2008.

[7] P. Pichat, "Partial or complete heterogeneous photocatalytic oxidation of organic compounds in liquid organic or aqueous phases," *Catalysis Today*, vol. 19, no. 2, pp. 313–333, 1994.

[8] M. A. Fox, "Organic heterogeneous photocatalysis: chemical conversions sensitized by irradiated semiconductors," *Accounts of Chemical Research*, vol. 16, no. 9, pp. 314–321, 1983.

[9] M. Kitano, M. Matsuoka, M. Ueshima, and M. Anpo, "Recent developments in titanium oxide-based photocatalysts," *Applied Catalysis A*, vol. 325, no. 1, pp. 1–14, 2007.

[10] J. Choi, H. Park, and M. R. Hoffmann, "Effects of single metal-ion doping on the visible-light photoreactivity of TiO_2," *Journal of Physical Chemistry C*, vol. 114, no. 2, pp. 783–792, 2010.

[11] A. Emeline, V. N. Kznetsov, V. K. Ryvchuk, and N. Serpone, "Visible-light-active titania photocatalysts: the case of N-doped TiO_2s—properties and some fundamental issues," *International Journal of Photoenergy*, vol. 2008, Article ID 258394, 19 pages, 2008.

[12] L. Samiolo, M. Valigi, D. Gazzoli, and R. Amadelli, "Photoelectro catalytic oxidation of aromatic alcohols on visible light-absorbing nitrogen-doped TiO_2," *Electrochimica Acta*, vol. 55, no. 26, pp. 7788–7795, 2010.

[13] Z. M. Dai, G. Burgeth, F. Parrino, and H. Kisch, "Visible light photocatalysis by a Titania-Rhodium(III) complex," *Journal of Organometallic Chemistry*, vol. 694, no. 7-8, pp. 1049–1054, 2009.

[14] H. Yu, H. Irie, and K. Hashimoto, "Conduction band energy level control of titanium dioxide: toward an efficient visible-light-sensitive photocatalyst," *Journal of the American Chemical Society*, vol. 132, no. 20, pp. 6898–6899, 2010.

[15] H. Irie, T. Shibanuma, K. Kamiya, S. Miura, T. Yokoyama, and K. Hashimoto, "Characterization of Cr(III)-grafted TiO_2 for photocatalytic reaction under visible light," *Applied Catalysis B*, vol. 96, no. 1-2, pp. 142–147, 2010.

[16] G. Colón, M. C. Hidalgo, J. A. Navío, A. Kubacka, and M. Fernández-García, "Influence of sulfur on the structural, surface properties and photocatalytic activity of sulfated TiO_2," *Applied Catalysis B*, vol. 90, no. 3-4, pp. 633–641, 2009.

[17] R. Murray, *Molecular Design of Electrode Surface*, John Wiley & Sons, New York, NY, USA, 1992.

[18] R. K. Grasselli, "Genesis of site isolation and phase cooperation in selective oxidation catalysis," *Topics in Catalysis*, vol. 15, no. 2-4, pp. 93–101, 2001.

[19] J. Haber, "Fifty years of my romance with vanadium oxide catalysts," *Catalysis Today*, vol. 142, no. 3-4, pp. 100–113, 2009.

[20] B. M. Weckhuysen and D. E. Keller, "Chemistry, spectroscopy and the role of supported vanadium oxides in heterogeneous catalysis," *Catalysis Today*, vol. 78, no. 1–4, pp. 25–46, 2003.

[21] M. Anpo, H. Yamashita, M. Matsuoka, D. R. Park, Y. G. Shul, and S. E. Park, "Design and development of titanium and vanadium oxide photocatalysts incorporated within zeolite

cavities and their photocatalytic reactivities," *Journal of Industrial and Engineering Chemistry*, vol. 6, no. 2, pp. 59–71, 2000.

[22] Y. Shiraishi, M. Morishita, Y. Teshima, and T. Hirai, "Vanadium-containing mesoporous silica of high photocatalytic activity and stability even in water," *Journal of Physical Chemistry B*, vol. 110, no. 13, pp. 6587–6594, 2006.

[23] R. Amadelli, A. Maldotti, and L. Samiolo, "Adsorption and photo-oxidation of 3,4-dihydroxy-cinnamic acid on TiO_2 films," *Catalysis Today*, vol. 144, no. 1-2, pp. 149–153, 2009.

[24] R. Mueller, H. K. Kammler, K. Wegner, and S. E. Pratsinis, "OH surface density of SiO_2 and TiO_2 by thermogravimetric analysis," *Langmuir*, vol. 19, no. 1, pp. 160–165, 2003.

[25] I. E. Wachs, "Raman and IR studies of surface metal oxide species on oxide supports: supported metal oxide catalysts," *Catalysis Today*, vol. 27, no. 3-4, pp. 437–455, 1996.

[26] Z. Luan and L. Kevan, "Electron spin resonance and diffuse reflectance ultraviolet-visible spectroscopies of vanadium immobilized at surface titanium centers of titanosilicate mesoporous TiMCM-41 molecular sieves," *Journal of Physical Chemistry B*, vol. 101, no. 11, pp. 2020–2027, 1997.

[27] I. E. Wachs and B. E. Weckhuysen, "On the surface structure of vanadia-titania catalysts: combined laser-Raman and fourier transform-infrared investigation," *Applied Catalysis A*, vol. 157, no. 1-2, pp. 67–90, 1997.

[28] I. E. Wachs, "In situ Raman spectroscopy studies of catalysts," *Topics in Catalysis*, vol. 8, no. 1-2, pp. 57–63, 1999.

[29] B. Olthof, A. Khodakov, A. T. Bell, and E. Iglesia, "Effects of support composition and pretreatment conditions on the structure of vanadia dispersed on SiO_2, Al_2O_3, TiO_2, ZrO_2, and HfO_2," *Journal of Physical Chemistry B*, vol. 104, no. 7, pp. 1516–1528, 2000.

[30] M. A. Bañares and I. E. Wachs, "Molecular structures of supported metal oxide catalysts under different environments," *Journal of Raman Spectroscopy*, vol. 33, no. 5, pp. 359–380, 2002.

[31] J. Zhang, M. Li, Z. Feng, J. Chen, and C. Li, "UV Raman spectroscopic study on TiO_2- I. phase transformation at the surface and in the bulk," *Journal of the Physical Chemistry B*, vol. 110, no. 2, pp. 927–935, 2006.

[32] R. S. Morrison, *Electrochemistry at Surface and Oxidized Metal Electrodes*, Plenum Press, New York, NY, USA, 1980.

[33] M. H. Dean and U. Stimming, "Capacity of semiconductor electrodes with multiple bulk electronic states. 2. Applications to amorphous semiconductor electrodes," *Journal of physical chemistry*, vol. 93, no. 24, pp. 8053–8059, 1989.

[34] D. Guyomard, "Basic principles of semiconductor electrochemistry," *Journal de Chimie Physique*, vol. 83, no. 6, pp. 355–391, 1986.

[35] J. Haber and P. Novak, "A catalysis related electrochemical study of the V_2O_5/ TiO_2(rutile) system," *Langmuir*, vol. 11, no. 3, pp. 1024–1032, 1995.

[36] J. M. Herrmann and J. Disdier, "Electrical properties of V_2O_5-WO_3/TiO_2 EUROCAT catalysts evidence for redox process in selective catalytic reduction (SCR) deNO_x reaction," *Catalysis Today*, vol. 56, no. 4, pp. 389–401, 2000.

[37] S. Takenaka, T. Tanaka, T. Funabiki, and S. Yoshida, "Reaction mechanism of photooxidation of propane over alkali-metal-ion-modified silica-supported vanadium pentaoxide under irradiation by visible light," *Journal of the Chemical Society*, vol. 93, no. 23, pp. 4151–4158, 1997.

[38] A. Z. Moshfegh and A. Ignatiev, "Photo-enhanced catalytic decomposition of isopropanol on V_2O_5," *Catalysis Letters*, vol. 4, no. 2, pp. 113–122, 1990.

[39] G. Busca, "FT-IR study of the surface chemistry of anatase-supported vanadium oxide monolayer catalysts," *Langmuir*, vol. 2, no. 5, pp. 577–582, 1986.

[40] S. Higashimoto, K. Okada, T. Morisugi et al., "Effect of surface treatment on the selective photocatalytic oxidation of benzyl alcohol into benzaldehyde by O_2 on TiO_2 under visible light," *Topics in Catalysis*, vol. 53, no. 7, pp. 578–583, 2010.

[41] V. Augugliaro, T. Caronna, V. Loddo et al., "Oxidation of aromatic alcohols in irradiated aqueous suspensions of commercial and home-prepared rutile TiO_2: a selectivity study," *Chemistry*, vol. 14, no. 15, pp. 4640–4646, 2008.

[42] A. Molinari, R. Amadelli, V. Carassiti, and A. Maldotti, "Photocatalyzed oxidation of cyclohexene and cyclooctene with $(nBU_4N)_4W_{10}O_{32}$ and $(nBu_4N)_4W_{10}O_{32}/Fe^{III}$[meso-tetrakis(2,6- dichlorophenyl)-porphyrin] in homogeneous and heterogeneous systems," *European Journal of Inorganic Chemistry*, vol. 2000, no. 1, pp. 91–96, 2000.

[43] G. R. Buettner, "Spin trapping: ESR parameters of spin adducts," *Free Radical Biology & Medicine*, vol. 3, no. 4, pp. 259–303, 1987.

[44] P. Pichat, M. Mozzanega, and H. Courbon, "Investigation of the mechanism of photocatalytic alcohol dehydrogenation over Pt/TiO_2 using poisons and labelled ethanol," *Journal of the Chemical Society Faraday Transactions 1*, vol. 83, no. 3, pp. 697–704, 1987.

[45] J. Chen, D. F. Ollis, W. H. Rulkens, and H. Bruning, "Kinetic processes of photocatalytic mineralization of alcohols on metallized titanium dioxide," *Water Research*, vol. 33, no. 5, pp. 1173–1180, 1999.

[46] Q. Wang and R. J. Madix, "Partial oxidation of methanol to formaldehyde on a model supported monolayer vanadia catalyst: vanadia on TiO_2(110)," *Surface Science*, vol. 496, no. 1, pp. 51–63, 2002.

[47] P. Ciambelli, D. Sannino, V. Palma, V. Vaiano, and R. S. Mazzei, "A step forwards in ethanol selective photo-oxidation," *Photochemical and Photobiological Sciences*, vol. 8, no. 5, pp. 699–704, 2009.

[48] T. Carlson and G. L. Griffin, "Photooxidation of methanol using V_2O_5/TiO_2 and MoO_3/TiO_2 surface oxide monolayer catalysts," *Journal of Physical Chemistry*, vol. 90, no. 22, pp. 5896–5900, 1986.

[49] M. L. Ganadu, L. Andreotti, I. Vitali, A. Maldotti, A. Molinari, and G. M. Mura, "Glucose oxidase catalyses the reduction of O_2 to H_2O_2 in the presence of irradiated TiO_2 and isopropyl alcohol," *Photochemical and Photobiological Sciences*, vol. 1, no. 12, pp. 951–954, 2002.

[50] G. Mul, W. Wasylenko, M. S. Hamdy, and H. Frei, "Cyclohexene photo-oxidation over vanadia catalyst analyzed by time resolved ATR-FT-IR spectroscopy," *Physical Chemistry Chemical Physics*, vol. 10, no. 21, pp. 3131–3137, 2008.

[51] V. N. Shetti, M. J. Rani, D. Srinivas, and P. Ratnasamy, "Chemoselective alkane oxidation by superoxo-vanadium(V) in vanadosilicate molecular sieves," *Journal of Physical Chemistry B*, vol. 110, no. 2, pp. 677–679, 2006.

[52] H. U. Blaser, H. Steiner, and M. Studer, "Selective catalytic hydrogenation of functionalized nitroarenes: an update," *ChemCatChem*, vol. 1, no. 2, pp. 210–221, 2009.

[53] H. Huang, J. Zhou, H. Liu, Y. Zhou, and Y. Feng, "Selective photoreduction of nitrobenzene to aniline on TiO_2 nanoparticles modified with amino acid," *Journal of Hazardous Materials*, vol. 178, no. 1–3, pp. 994–998, 2010.

[54] S. O. Flores, O. Rios-Bernij, M. A. Valenzuela, I. Córdova, R. Gómez, and R. Gutiérrez, "Photocatalytic reduction of

nitrobenzene over titanium dioxide: by-product identification and possible pathways," *Topics in Catalysis*, vol. 44, no. 4, pp. 507–511, 2007.

[55] A. Maldotti, R. Amadelli, L. Samiolo et al., "Photocatalytic formation of a carbamate through ethanol-assisted carbonylation of p-nitrotoluene," *Chemical Communications*, no. 13, pp. 1749–1751, 2005.

[56] A. Corma, P. Serna, P. Concepción, and J. J. Calvino, "Transforming nonselective into chemoselective metal catalysts for the hydrogenation of substituted nitroaromatics," *Journal of the American Chemical Society*, vol. 130, no. 27, pp. 8748–8753, 2008.